Thermal and rheological properties and processability of thermoplastic lignocellulose

Received: 1 April 2024 | Revised: 21 June 2024 | Accepted: 23 June 2024

DOI: 10.1002/app.55958

RESEARCH ARTICLE

Applied Polymer SCIENCE WILEY

Thermal and rheological properties and processability of thermoplastic lignocellulose

Bahiru Tsegaye[1,2,3] | **Kristofer Westerberg**[4] | **Anna Ström**[1,2] | **Mikael S. Hedenqvist**[2,3]

[1]Applied Chemistry, Department of Chemistry and Chemical Engineering, Chalmers University of Technology, Göteborg, Sweden

[2]FibRe-Center for Lignocellulose-based Thermoplastics, Department of Chemistry and Chemical Engineering, Chalmers University of Technology, Göteborg, Sweden

[3]Department of Fibre and Polymer Technology, School of Engineering Sciences in Chemistry, Biotechnology and Health, KTH Royal Institute of Technology, Stockholm, Sweden

[4]IV Frohe Sweden AB, Tyresö, Sweden

Correspondence
Bahiru Tsegaye, Applied Chemistry, Department of Chemistry and Chemical Engineering, Chalmers University of Technology, Kemivägen 10, SE-41296, Göteborg, Sweden.
Email: bahiru@chalmers.se

Funding information
VINNOVA, Grant/Award Number: 2019-00047

Abstract

Fossil-free biobased materials like thermoplastic lignocellulose are gaining attention because of climate issues. However, there is a challenge to make these as thermoplastic as commonly used thermoplastics. Arboform® is one of today's commercially available thermoplastic lignocellulose materials. In this work, the processability of this material was studied in detail and the effects of plasticizers on its processability, rheological, and mechanical properties were determined. Thermal/calorimetry analysis indicated that the processing temperature window was shifted to lower temperature with the use of tributyl citrate (TBC) and poly(ethylene glycol) (PEG 400) plasticizers, thus enabling extrusion at lower temperature. TBC and PEG 400 decreased both the glass transition temperature and melting point of the polylactide component. Surprisingly, they also affected the lignin component, as observed by the decreasing lignin decomposition temperature. It is observed that TBC and PEG400 lowered the stiffness of the compression molded material in the temperature range investigated (−30–180°C), and tensile tests in the presence of TBC revealed a decrease in ductility. Notable is that, in contrast to most thermoplastics, the Arboform® melt increases in viscosity and elastic moduli when the processing temperature was increased (from 180 to 200°C) or when processing time was increased.

KEYWORDS

biopolymers and renewable polymers, extrusion, plasticizer, rheology, thermoplastics

1 | INTRODUCTION

Plastic pollution is one of the main problems facing the world and it is recognized as a serious environmental problem by United Nations environmental assembly.[1] Conversely, the demand for plastics is on the rise, having reached 390.7 million metric tons in 2021 and is anticipated to triple by 2050.[2,3] This has led the United Nations (UN) to adopt a resolution working toward ending plastic pollution and a legal global binding agreement has been initiated, slated for implementation in 2024.[1] The trend in plastic consumption and pollution shows the need to move toward renewable and sustainable material production by decoupling from fossil-based materials.

In recent years, interest in developing different sustainable materials from lignocellulose biomass has grown rapidly. Thermoplastic lignocellulose materials have been produced from for example, wheat straw,[4] wheat bran,[5] sugarcane bagasse,[6–8] wood pulps,[9–12] mulberry,[9,13] and eucalypt wood powder.[14] Given the heterogeneity of lignocellulose biomass, the development of thermoplastic materials from lignocellulose biomass is still challenging. However, some thermoplastic lignocellulose materials have been successfully commercialized. Arboform®, also known as "liquid wood," is among these materials. It is a multicomponent material with a density of 1.3 g/cm^3 and is composed of lignin, naturally occurring fibers, and various biobased additives, such as polylactide.[15–17] It can be used for loudspeaker boxes, gift boxes, and other esthetic and design objects.[18] Lignin acts as a binder and matrix[18] while the natural fiber reinforces the system. The unique composition of Arboform®, its lignocellulose nature, inspired us to use it as a model thermoplastic lignocellulose material to study the melt processability and effects of plasticizers/processing aids.

Nedelcu et al., reported a detailed mechanical and thermal characterization of Arboform LV3. They observed two thermal transitions: an endothermal region between room temperature and 77°C, followed by an exothermal region after 77°C.[17,19] They reported a toughness of 8.5 × 10^3 J/m^2, a tensile strength of 61 MPa and recyclability without losing the thermal properties.[20] Results from nanoindentation revealed that the hardness increased from 195 to 350 MPa with a rise in processing temperature.[21] Arboblend® also shows increased hardness and elastic modulus with increasing processing temperature from 160 to 170°C.[22]

Blends of Arboform and polypropylene (PP) and poly(butylene succinate) (PBS) were studied.[23,24] The tensile strength of PBS increased tenfold when blended with 65% Arboform®. However, a highly viscous composite melt was observed, which was suggested to be due to lignin crosslinking.[23] The tensile modulus of the composite increased with increasing Arboform® content, attributed to polar–polar interaction between the lignin component and the polyesters.[23]

Although results from laboratory have demonstrated that flowable and thermoplastic materials can be developed from lignocellulose biomass, studies on the impact of processing conditions and additives/processing aids on the processability of modified materials are less understood.

Hence, the aim of this work was to investigate the effects of processing parameters and plasticizers/lubricants on the processability, rheology, mechanical, and thermal properties of Arboform® (thermoplastic lignocellulose material). The influence of processing conditions and the effect of plasticizers on the mechanical properties, rheological properties, and thermal properties were investigated using thermogravimetry (TGA), differential scanning calorimetry (DSC), dynamic mechanical analysis (DMA), Fourier transform infrared spectroscopy (FTIR), scanning electron microscopy (SEM), rheology, and tensile testing.

2 | MATERIALS AND METHODS

2.1 | Chemicals and materials

Arboform (Arboform® LV 100B) was kindly provided by Albis Nordics & Baltics AB (Göteborg, Sweden). According to the manufacturer, Arboform is made from 100% renewable raw materials and it is biodegradable.[25] Glycerol with a purity of ≥99%, tributyl citrate (TBC) with a purity of ≥97% and poly (ethylene glycol) 400 (PEG 400) were purchased from Sigma-Aldrich and used as is.

2.2 | Sample preparations

Arboform® was dried at 50°C for 24 h in an oven prior to any processing and analysis. Just before extrusion, it was ground using a hammer mill with 0.5 mm sieve and manually mixed with plasticizer (glycerol, TBC or PEG 400). To reduce the impact of temperature during milling, Arboform® pellets were soaked in liquid N_2 for 1–2 min immediately before milling.

2.3 | Melt processing and plasticization of Arboform

A corotating lab scale twin-screw extruder (Xplore MC 5 Micro compounder, Netherland) was used for compounding the ingredients. Glycerol (molecular weight, 92 g/mol), TBC (molecular weight, 360 g/mol), and PEG 400 (molecular weight 400 g/mol) were used as plasticizer with a weight ratio of 3%, 5%, 10%, 15%, 20%, 25%, and 30%. The compounding was performed at a temperature of 170°C and screw speed of 50 rpm for an extrusion time of 5 min. The different ingredients were mixed manually just before extrusion and then immediately added into the extruder. The extrusion time was established from the time all mixtures were fed into the extruder to when the outlet valve opened.

All the extrudates and neat Arboform® samples were compression molded at 170°C with an applied force of 150 kN for 10 min using a compression molding machine (Fontijne presses BV, Netherland) into different geometries for different measurements. For shear viscosity measurements circular specimens were produced (4 mm

thickness and 25 mm diameter) and rectangular specimens were produced for DMA ($1 \times 10 \times 30$ mm^3) and for tensile tests ($2 \times 12 \times 60$ mm^3).

2.4 | Characterizations of all samples

2.4.1 | Microstructure and water contact angle analysis

The cross-sections of the Arboform® pellets were analyzed by scanning electron microscopy (SEM, JOEL 7800F Prime instrument) at an accelerated voltage of 3 kV. A hammer was used to break the pellets for a cross-sectional view. The water contact angle was measured by the sessile droplet method using an Attention Theta optical tensiometer (Biolin, Finland). About 2 μL water droplet size was placed onto the surface with the help of a microsyringe and the water contact angle was measured by capturing the images of the droplet every 10 s.

2.4.2 | Thermal properties

The thermal stability and phase transitions of the neat and plasticized Arboform® were analyzed by DSC (Mettler Toledo DSC2 instrument), TGA (Mettler Toledo TGA/DSC3+), and DMA (Q800, TA Instrument). DSC experiments were conducted by placing approximately 10 mg of the samples in aluminum crucibles. The samples were heated from −70 to 200°C under a N_2 atmosphere with a purge gas rate of 50 mL/min using a 10°C/min heating rate. The fictive temperature was used to determine the glass transition temperature (T_g) (Gedde & Hedenqvist, 2019). TGA was performed by adding approximately 10 mg of sample in ceramic crucibles and heating these from 25 to 800°C under N_2 atmosphere with a purge gas rate of 50 mL/min.

DMA measurements were carried out in tension mode at constant frequency (1 Hz) with a heating scan from −130 to 190°C (or until a substantial softening of the material occurred) at a heating rate of 5°C/min. For every sample, three replicates were prepared and measured. Loss modulus (E'') was used to determine T_g from the DMA plots, tangent lines were drawn when one magnitude drop in E'' was observed and the intersection points of the tangent lines were used as T_g.

2.4.3 | Shear rheology

A rotational rheometer (DHR3, TA Instruments) equipped with an oven was used for analysis of the rheological properties of the samples (storage modulus (G'), loss modulus (G''), and loss factor [tan δ]). A plate–plate geometry was used. Oscillation strain amplitude sweeps were done at constant frequency of 1 Hz and strain sweep from 0.01% to 60%, frequency sweeps were done at a frequency range from 0.01 to 100 Hz at a constant strain amplitude of 0.5%, time sweeps were done at constant frequency of 1 Hz and a strain amplitude of 0.5%. The temperatures used were 180, 190, and 200°C. All samples were conditioned at the set temperature for 3 min before the time sweeps started, and all experiments were conducted under ambient air atmosphere.

2.4.4 | Mechanical properties

Tensile tests were performed using universal testing machine (Mechanical tester Instron 5565A) with a 5 kN load cell and a crosshead speed of 10 mm/min. The tests were performed using a gauge length of 30 mm at room temperature and relative humidity of 27%.

3 | RESULTS AND DISCUSSIONS

3.1 | Assessment of processability of Arboform

Figure 1 shows the T_m, T_g, and T_d (onset decomposition temperature) of neat Arboform® obtained with DMA, DSC, and TGA. The temperature range between T_m and T_d defines the processing window.[7,26,27] Arboform® shows a melting between ca. 160 and 180°C, with a melting peak temperature (T_m) at 173°C and a T_g of 51°C (fictive temperature from DSC), both referring to the PLA component (Figure 1a).[15] T_d, as determined from the onset of significant mass loss, was 265°C (Figure 1).

The DMA results show a broad shoulder in the glassy region spanning from around −100 to 20°C that is possibly a sub glass transition, considering that the stiffness is above 3 GPa above this transition.[28] The T_g, obtained with DMA, was determined to be around 73–75°C (Figure 1b). It is not uncommon to observe a significant difference (as much as 25°C) in T_g's obtained from DMA and DSC,[29,30] especially for complex structures, such as those of lignocellulose materials. The difference in T_g obtained from DSC and DMA is due to the nature of the measurement. The change in heat capacity (by DSC) does not necessarily coincide with a dramatic change in the molecular mobility (observed with DMA). Mechanical relaxation, thermal hysteresis, and sample size are factors that may affect the position of the measured T_g. A higher strain frequency will also decrease the DMA measured

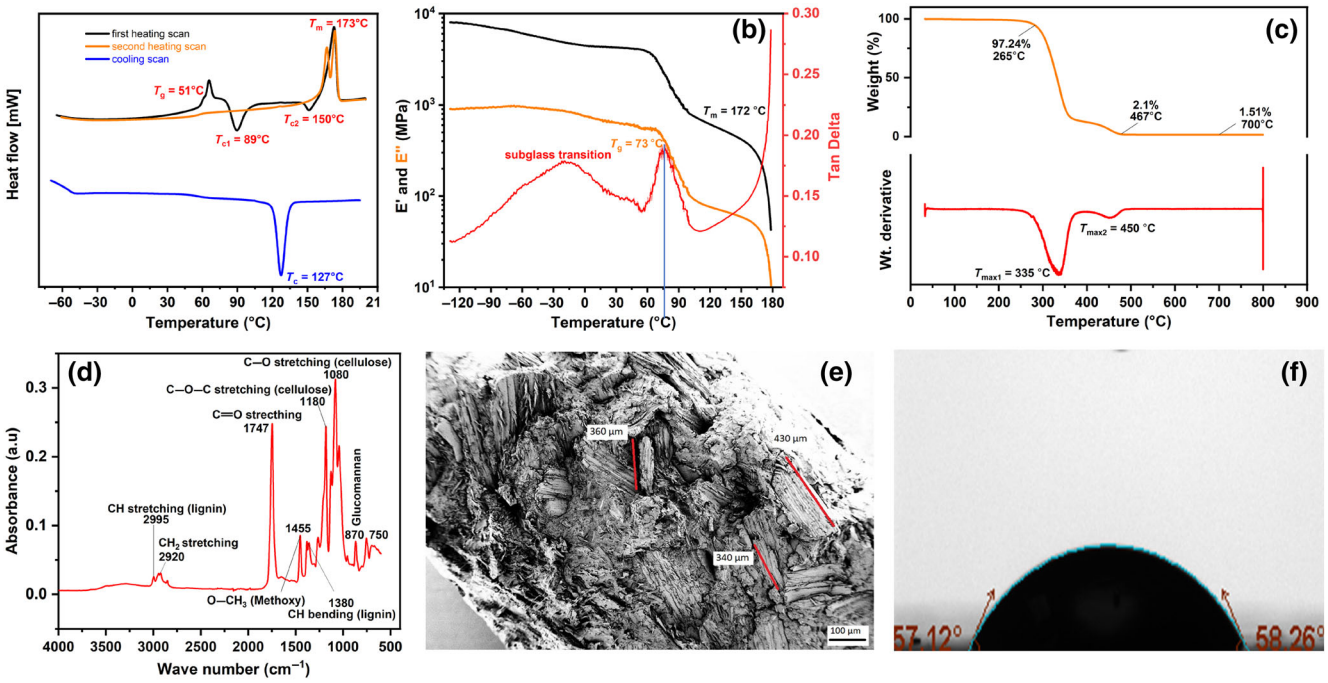

FIGURE 1 Thermal properties as determined using (a) DSC, (b) DMA, (c) TGA, (d) FTIR, (e) microstructure as visualized using SEM, and (f) water contact angle. DMA, dynamic mechanical analysis; DSC, differential scanning calorimetry; FTIR, Fourier transform infrared spectroscopy; TGA, thermogravimetry. [Color figure can be viewed at wileyonlinelibrary.com]

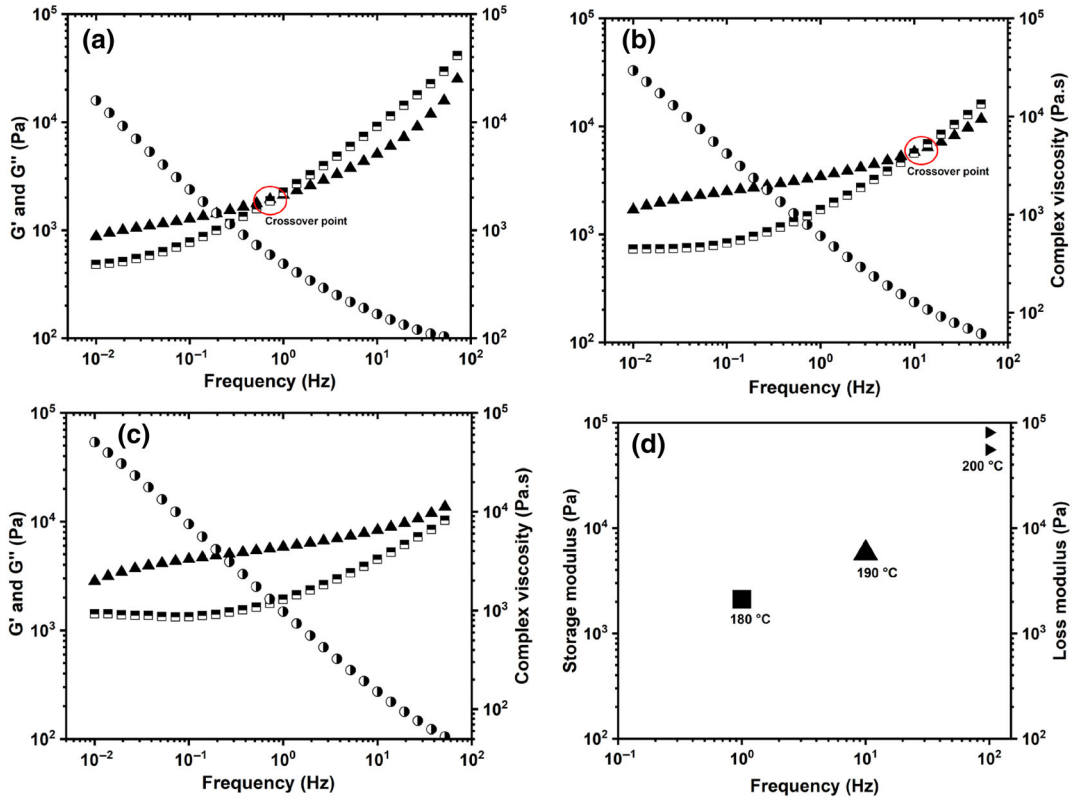

FIGURE 2 G' (triangles), G'' (squares), and complex viscosity (circles) as a function of frequency at: (a) 180°C, (b) 190°C, (c) 200°C. In (d) the G′ and G″ are given at the frequency where G′ = G″. [Color figure can be viewed at wileyonlinelibrary.com]

transition toward the DSC obtained T_g. It is also evident, from the DSC plot (Figure 1a), that the PLA component had two distinct cold crystallization points (at 89 and 150°C), suggesting the presence of different crystalline phases. TGA (Figure 1c) shows a large mass loss between 250 and 340°C due to thermal degradation of hemicellulose and cellulose and a smaller loss between 360 and 470°C, which is due to thermal degradation of lignin (Figure 1c). The relatively large difference in T_m and T_d indicated a relatively large processing temperature window. Note that we are using the melting peak as the lower limit, but the material was processable/extrudable from the onset of melting (160°C), although the extrusion was more difficult to perform at 160°C than at higher temperature.

The presence of absorption bands assigned to hemicellulose, cellulose, and lignin were observed in the FTIR spectra (Figure 1d). Absorption bands at 1180 and 1080 cm^{-1} refer to unsymmetric and symmetric stretching vibration of C—O—C in cellulose, respectively, 870 cm^{-1} to b-glycosidic linkage vibrations hemicellulose and 2980/1380 cm^{-1} corresponds to C—H stretching and bending vibrations, respectively, in aromatic ring structure of lignin. The absorbance in the ~3700–3200 cm^{-1} region is due to hydroxyl groups (mainly cellulose and hemicellulose) and the 1747 cm^{-1} band originates from the polyester (PLA) component.[31–33]

Figure 1e,f show a SEM micrograph of Arboform and the water contact angle of hot pressed Arboform. SEM revealed randomly oriented fiber fragments throughout the matrix, with sizes ranging from 280 to 430 μm in length and 20–80 μm in width. These contribute to the strength, hardness, and stiffness of the composite, but also to reduced ductility and brittleness. The water contact angle was 57°, which shows the hydrophilic nature of Arboform. A water contact angle of 57° is for example lower than PLA (≈67°).[8]

TABLE 1 Viscoelastic properties (G' and tan δ) of Arboform® determined at a frequency of 1 Hz at $t = 10$ and 30 min.

	$t = 10$ min		$t = 30$ min	
T/°C	G'/Pa	Tan δ	G'/Pa	Tan δ
180	2160	1.5	2590	1.1
190	2380	1	3180	0.6
200	3220	0.7	4850	0.4

3.2 | Rheological properties

Figure 2a–c show the frequency dependence of the viscoelastic properties of Arboform® at various temperatures (180, 190, and 200°C). The frequency sweep at 180°C shows more elastic ($G' > G''$) behavior at lower frequencies (0.01–1 Hz) and a more viscous behavior ($G' < G''$) at higher frequencies (1–100 Hz), (Figure 2a). Such behavior (shift from predominant elastic to viscous behavior upon increase in frequency) is usually observed in viscoelastic solids.[34–36] As temperature increased to 190°C (Figure 2b), the solid/elastic like behavior dominated over a larger frequency region (0.01–10 Hz), and at 200°C (Figure 2c), it dominated over the whole frequency range studied (0.01–100 Hz). Consequently, as the temperature increased, the crossover point ($G' = G''$) shifted at higher frequency (Figure 2d). Hence, Arboform, in contrast to common thermoplastic polymers, showed a more elastic or solid like behavior at higher temperature. In addition,

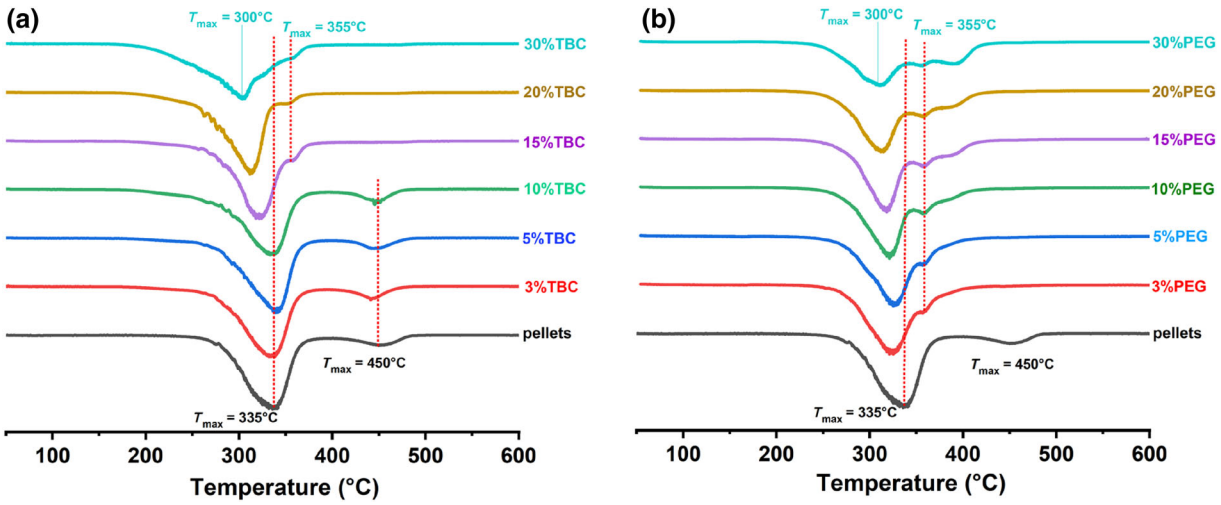

FIGURE 3 Thermal stability of TBC-Arboform® (a) and PEG-Arboform® (b) blends from derivative of thermogravimetric analysis (DTGA) curves (d_m/d_T vs. T). PEG 400, poly(ethylene glycol); TBC, tributyl citrate. [Color figure can be viewed at wileyonlinelibrary.com]

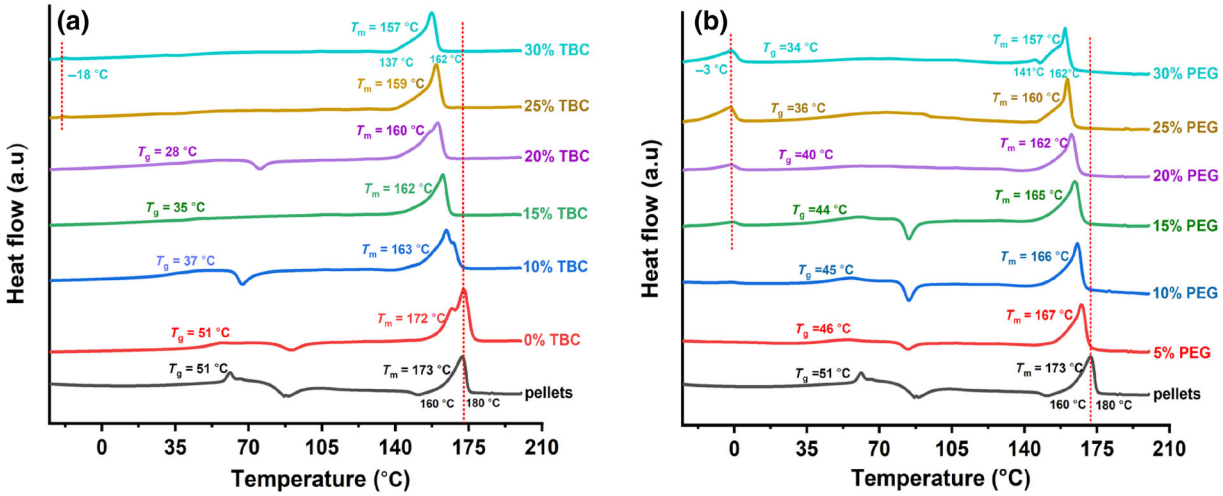

FIGURE 4 DSC plots of Arboform® containing different amounts of (a) TBC and (b) PEG 400. PEG 400, poly(ethylene glycol); TBC, tributyl citrate. [Color figure can be viewed at wileyonlinelibrary.com]

TABLE 2 Thermal properties of Arboform® with TBC and PEG 400.

Sample	T_g (°C)	T_m (°C)	T_d (°C)	Processing window (°C)[a]
Arboform®	51	173	265	92
3% TBC	39	167	217	50
5%	37	166	217	51
10%	37	163	213	50
15%	35	162	213	51
20%	28	160	206	46
25%	-	159	200	41
30%	-	157	200	43
3% PEG 400	48	168	250	82
5%	46	167	250	83
10%	45	166	245	79
15%	44	165	240	75
20%	40	162	237	75
25%	36	160	235	75
30%	34	157	225	68

Abbreviations: PEG 400, poly(ethylene glycol); TBC, tributyl citrate.
[a]Defined here as the difference between T_m and T_d.

the storage modulus G′ increased also in absolute values with increasing temperature from 180 to 200°C.

Time sweep measurements performed at different temperatures and summarized in Table 1 (with specific focus on G' and tan delta at time = 10 and 30 min), further confirmed the increase in absolute value of G' with increasing temperature. G' also increased in absolute value with increasing time, as shown by the increase in G' obtained between $t = 10$ and 30 min (Table 1). In addition, tan δ, decreased with increase in temperature and time, confirming stiffening of the material. The temperature and time-induced stiffening of the material suggest that a chemical process is responsible for this, possibly a crosslinking process or repolymerization of the lignin component.[23] We rule out oxidation being the reason for the stiffening, since similar rheological behavior was observed in air and nitrogen (time sweep data, not shown). The results show that the melt processability of Arboform® can be affected negatively by longer processing time at elevated temperature (above 190°C). Further investigation is needed to determine the exact reason for the stiffening of Arboform® as a function of time and temperature.

Due to the distinct rheological properties dependence on temperature and time, compared to purely viscoelastic

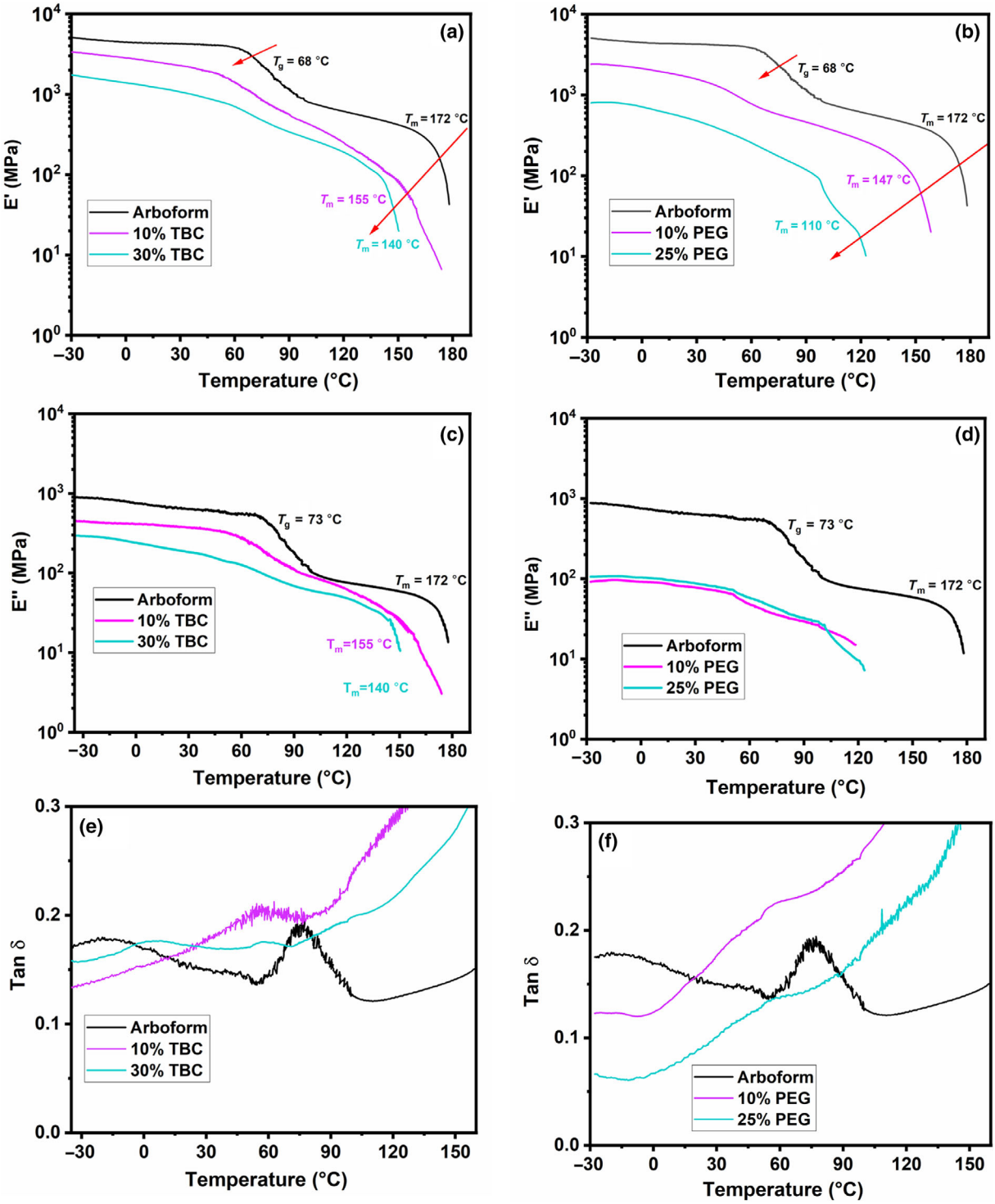

FIGURE 5 DMA plots of Arboform® modified with TBC (a, c, and e) and PEG 400 (b, d, and f) as measured at frequency of 1 Hz and strain of 0.05%. DMA, dynamic mechanical analysis; PEG 400, poly(ethylene glycol); TBC, tributyl citrate.

The tensile tests showed, in accordance with the DMA data, that the modulus/stiffness decreased in the presence of TBC. However, the ductility (strain at break) also decreased, leading to also a lower strength (fracture stress) (Figure 6). Based on the similarity of the DSC and DMA results of the TBC and PEG 400, it was not meaningful to perform tensile tests on the PEG 400 system. The general appearance was a similar embrittlement in both plasticizer systems. This behavior is not uncommon in composites/filled polymer systems.[26,41–43] Since, the stiffness was reduced when adding the plasticizer (refer to both tensile and DMA data), the bonding is not improved between the fibers. The plasticizer plasticizes the PLA component and is also affecting the lignin component (which acts as a glue for the fibers). This reduces the bonding of the fibers, reduces the strength and facilitates an earlier fracture (reduced strain at break). [Color figure can be viewed at wileyonlinelibrary.com]

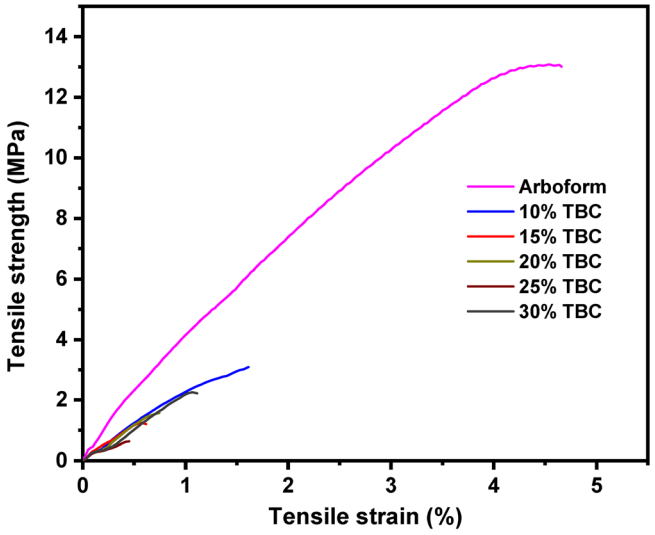

FIGURE 6 Representative stress–strain curves of TBC modified Arboform®. TBC, tributyl citrate. [Color figure can be viewed at wileyonlinelibrary.com]

thermoplastics, the latter experiencing a decreasing stiffness, and viscosity with increasing temperature, the generation of a master curve was expected to fail.[37–39] Indeed, it was not possible to shift the rheological and moduli data to a single master curve (Figure S1). Consequently, the moduli and viscosity did not follow an Arrhenius curve with a single activation energy.[40]

3.3 | Compatibility between Arboform and glycerol

Glycerol turned the light brown Arboform to a black color at the processing temperatures, which indicated a reaction with Arboform. Its ability to plasticize Arboform® was also absent, and no further investigation of the glycerol-Arboform® system was therefore made.

3.4 | Thermal and mechanical properties of modified Arboform

The thermal properties, as revealed by the rate of mass loss in the TGA experiment of Arboform® containing TBC and PEG400, are shown in Figure 3. The maximum mass loss rate occurred at 335°C for neat Arboform®, with a second peak due to lignin degradation at 450°C. The peak positions were the same from 0 to 10 wt.% TBC. At 15 wt.% TBC and higher, the major peak shifted toward lower temperature, which was probably originating from the combination of TBC evaporation and cellulose/hemicellulose degradation. Interestingly, in the same higher TBC content, the lignin maximum mass loss rate peak disappeared at 450°C and reappeared at 355°C. Hence, TBC affected the thermal stability of the lignin. On the other hand, the major peak in mass loss rate in the PEG 400 Arboform® system shifted to lower temperature already in the presence of 3 wt.% PEG 400. At the same low PEG 400 content, the lignin peak reappeared at the same lower temperature as for TBC (355°C). However, signs of a shoulder at 390°C were also observed from 3 wt.% and higher of PEG 400. In fact, it developed to a peak at higher PEG 400 content. This was possibly associated with lignin degradation.

As in the TGA data, TBC and PEG 400 induced changes in the calorimetric properties of Arboform®, which referred to the PLA component (Figure 4). The neat Arboform® pellets showed a clear T_g (fictive temperature) at 51°C, cold crystallization (T_c) peaking at ~85 and 160°C, before melting with a peak at 173°C. The extruded neat Arboform® had a similar T_g and first T_c as the pellets (Figure 4a). However, the second T_C (at higher temperature) was not observed, and the main T_m was observed at 172°C. A smaller melting peak was observed at 158°C, indicating two different PLA crystal populations with different crystal thicknesses. As the TBC content was increased the T_g decreased but became also more difficult to observe. For the 25 and 30 wt.% TBC, the T_g could not be observed in the DSC curves. The melting temperature region was also shifting to lower temperature with increasing TBC content. Hence, TBC reduced the thermal stability of the PLA crystals. The same was also observed in the presence of PEG 400. Both the PLA melting region shifted to lower temperature and the T_g decreased with increasing PEG 400 content (Figure 4b). In both the TBC and PEG 400 systems, some phase separation between Arboform and TBC/PEG 400 occurred at the highest TBC/PEG 400 content, as indicated by a T_m at −18°C (TBC) and −3°C (PEG 400). The T_g and T_m of PLA from DSC and the composite degradation temperature from TGA, and the corresponding processing window (between the PLA T_m and composite T_d) are summarized in Table 2. Noteworthy is that the presence of TBC and PEG 400 shifted the processing temperature window to lower temperature.

To further analyze the thermal transitions in the presence of TBC and PEG400, DMA was performed. It was clearly observed that both TBC and PEG 400 reduced the storage modulus (E') over the whole temperature region, that is, up to the melting region, or sample fracture (where the modulus had decreased to ~10–20 MPa). Hence, both TBC and PGA 400 had a clear plasticizing effect on the Arboform® material. As shown above, the two chemicals plasticized PLA, but as shown in the TGA data, they also affected the thermal properties of the

lignin component. The lower E' at room temperature in the PEG 400 system, compared to the TBC system, indicated a higher degree of plasticization/softening with PEG 400 (Figure 5a,b). However, as shown above, the reduction in the DSC T_g of the PLA phase was stronger with TBC, indicating a stronger plasticization by TBC on the PLA component. However, the effects on the lignin component (refer to the TGA data) started to occur at a lower PEG 400 content than in the TBC case. Hence, the effects of TBC/PEG 400 on the mechanical properties seemed to be a combination of mechanisms occurring in both the PLA and lignin phases.

4 | CONCLUSIONS

Lignocellulose materials are generally difficult to process using techniques like extrusion and injection molding. Arboform®, however, is readily processable using extrusion. The rheological data showed that an increasing melt temperature (from 180 to 200°C) or extended processing time increased the storage modulus of the melt. In addition, the frequency range within which the elastic behavior dominated over the viscous behavior increased, suggesting a chemical reaction taking place.

Glycerol was found unsuitable as a plasticizer, despite the hydrophilic nature of the material. In contrast, the less hydrophilic and larger plasticizers TBC and PEG400 effectively reduced the stiffness of Arboform®. TBC and PEG400 also affected the lignin component, as observed by the decrease in the lignin decomposition temperature. The two plasticizers had somewhat different effects on the Arboform® properties. The PEG 400 system showed greater plasticization/softening of the whole composite, indicated by the lower E' at room temperature. PEG 400 had also stronger effects on the lignin component. However, the reduction in the DSC-determined T_g of the PLA phase was stronger with the ester (TBC), indicating a stronger plasticization by TBC of the PLA component. As often observed for composite materials, the plasticization/softening led to decreased strain at break (ductility). Besides the decrease in T_g induced by plasticization, both plasticizers similarly decreased the melting temperature of the PLA component. This enables extrusion and processing of the composite at a lower temperature.

This work shows that it is possible to enhance the properties of a lignocellulose material (having a large amount of cellulose fiber fillers) by selecting suitable plasticizers. However, the mechanisms are complex due to the composite structure, and the type of plasticizer can affect the different components of the composite in different ways and/or to different extents. Hence, conducting comprehensive studies on the impact of plasticizer and the processability of thermoplastic lignocellulose materials are essential.

AUTHOR CONTRIBUTIONS

Bahiru Tsegaye: Conceptualization (equal); data curation (lead); visualization (lead); writing – original draft (lead); writing – review and editing (equal). **Kristofer Westerberg:** Conceptualization (equal); data curation (equal); supervision (equal); writing – review and editing (equal). **Anna Ström:** Conceptualization (equal); data curation (equal); funding acquisition (lead); supervision (equal); writing – review and editing (equal). **Mikael S. Hedenqvist:** Conceptualization (equal); data curation (equal); funding acquisition (lead); supervision (lead); writing – review and editing (equal).

ACKNOWLEDGMENTS

This work is funded by Fiber—Design for Circularity: Lignocellulose-based Thermoplastics (grant number 2019-00047), a VINNOVA competence center.

CONFLICT OF INTEREST STATEMENT

The authors declare that they have no known competing financial interests or personal relationships that could have appeared to influence the work reported in this paper.

DATA AVAILABILITY STATEMENT

The data that support the findings of this study are available in thesupplementary material of this article.

ORCID

Bahiru Tsegaye https://orcid.org/0000-0002-5145-5772

REFERENCES

[1] EA. 5/Res, 14 UNEP, *Resolution adopted by the United Nations Environment Assembly on 2 March 2022 5/14.*, UNITED NATIONS: Nairobi, 2022, pp 3.
[2] Statista, global plastic production **1950**-1921https://www.statista.com/statistics/282732/global-production-of-plastics-since-1950/ (accessed May 23, 2023).
[3] R. Geyer, J. R. Jambeck, K. L. Law, *Sci. Adv.* **2017**, *3*, 25.
[4] J. Chen, M. Su, J. Ye, Z. Yang, Z. Cai, H. Yan, J. Hong, *Polym. Compos.* **2014**, *35*, 419.
[5] M. Börjesson, G. Westman, A. Larsson, A. Ström, *ACS Appl. Polym. Mater.* **2019**, *1*, 1443.
[6] S. Suzuki, H. Hikita, S. C. Hernandez, N. Wada, K. Takahashi, *ACS Sustain. Chem. Eng.* **2021**, *9*, 5933.
[7] S. Suzuki, Y. Hamano, S. C. Hernandez, N. Wada, K. Takahashi, *ACS Sustain. Chem. Eng.* **2021**, *9*, 15249.
[8] T. Li, Y. Zhang, Y. Jin, L. Bao, L. Dong, Y. Zheng, J. Xia, L. Jiang, Y. Kang, J. Wang, *J. Cleaner Prod.* **2023**, *386*, 135834.
[9] X. Li, J. Ye, J. Hong, Y. Fu, *Eur. J. Wood Wood Prod.* **2022**, *80*, 923.

[10] J. Li, T. Baker, G. G. Sacripante, D. J. W. Lawton, H. S. Marway, H. Zhang, M. R. Thompson, *Carbohydr. Polym.* **2021**, *270*, 118361.
[11] J. Li, H. Zhang, G. G. Sacripante, D. J. W. Lawton, H. S. Marway, M. R. Thompson, *Cellulose* **2021**, *28*, 1055.
[12] J. Li, D. J. W. Lawton, G. G. Sacripante, M. R. Thompson, H. S. Marway, *Ind. Eng. Chem. Res.* **2021**, *60*, 13886.
[13] J. Chen, C. Tang, Y. Yue, W. Qiao, J. Hong, T. Kitaoka, Z. Yang, *Ind. Crops Prod.* **2017**, *108*, 286.
[14] C. Tian, M. Yan, X. Huang, Y. Zhong, H. Lu, X. Zhou, *Cellulose* **2022**, *29*, 1487.
[15] I. Blanco, G. Cicala, A. Latteri, G. Saccullo, A. M. M. El-Sabbagh, G. Ziegmann, *J. Therm. Anal. Calorim.* **2017**, *127*, 147.
[16] N. Helmut, J. Pfitzer, E. Nägele, E. R. Inone, W. E. Norbert Eisenreich, P. Eyerer, in *Chemical Modifications, Properties, and Usage of Lignin* (Ed: T. Q. Hu), Springer Science+Business Media, LLC, New York **2002**.
[17] D. Nedelcu, N. M. Lohan, I. Volf, R. Comaneci, *Composites, Part B* **2016**, *103*, 84.
[18] H. Nagele, J. Pfitzer, L. Ziegler, E. R. Inone-Kauffman, W. Eckl, N. Eisenreich, *Bio-Based Plastics*, John Wiley & Sons, Ltd, Karlsruhe, Germany **2014**, p. 91.
[19] D. Nedelcu, C. Ciofu, N. M. Lohan, *Composites, Part B* **2013**, *55*, 11.
[20] D. Nedelcu, L. Santo, A. G. Santos, S. P. Mazurchevici, *Mater. Plast.* **2015**, *52*, 423.
[21] E. Broitman, D. Nedelcu, S. Mazurchevici, H. Glenat, S. Grillo, *J. Tribol.* **2019**, *141*, 141.
[22] E. Broitman, D. Nedelcu, S. N. Mazurchevici, *E-Polym.* **2020**, *20*, 528.
[23] S. Sahoo, M. Misra, A. K. Mohanty, *Composites, Part A* **2011**, *42*, 1710.
[24] G. Cicala, C. Tosto, A. Latteri, A. D. La Rosa, I. Blanco, A. Elsabbagh, P. Russo, G. Ziegmann, *Materials* **2017**, *10*, 10.
[25] TECNARO, TECNARO The Biopolymer Company. https://www.tecnaro.de/en/arboblend-arbofill-arboform/ (accessed May 12, 2023).
[26] R. T. Umemura, M. I. Felisberti, *J. Appl. Polym. Sci.* **2021**, *138*, 1.
[27] B. Tsegaye, A. Ström, M. S. Hedenqvist, *Carbohydr. Polym. Technol. Appl.* **2023**, *5*, 2666.
[28] K. Dyamenahalli, A. Famili, R. Shandas, *Characterization of shape-memory polymers for biomedical applications*, Elsevier Ltd., Cambridge, UK **2015**.
[29] K. P. Menard, N. R. Menard, *Encyclopedia of Polymer Science and Technology*, Wiley, Hoboken, NJ **2015**, p. 1.
[30] L. De Nardo, S. Farè, *Charact. Polym. Biomater.* **2017**, 1, 203.
[31] M. Maiza, M. T. Benaniba, V. Massardier-Nageotte, *J. Polym. Eng.* **2016**, *36*, 371.
[32] M. P. Arrieta, J. López, E. Rayón, A. Jiménez, *Polym. Degrad. Stab.* **2014**, *108*, 307.
[33] J. Gálvez, J. P. Correa Aguirre, M. A. Hidalgo Salazar, B. V. Mondragón, E. Wagner, C. Caicedo, *Polymer* **2020**, *12*, 2111.
[34] R. Srisuk, L. Techawinyutham, S. Mavinkere Rangappa, S. Siengchin, R. Dangtungee, *Polym. Compos.* **2020**, *41*, 5082.
[35] L. Techawinyutham, W. Techawinyutham, S. Mavinkere, *Int. J. Biol. Macromol.* **2024**, *257*, 128767.
[36] M. Žiganova, R. Merijs-Meri, J. Zicāns, I. Bochkov, T. Ivanova, A. Vīgants, E. Ence, E. Štrausa, *Polymer* **2023**, *15*, 2896.
[37] R. Li, *Mater. Sci. Eng., A* **2000**, *278*, 36.
[38] D. Ionita, M. Cristea, C. Gaina, *Polym. Test.* **2020**, *83*, 106340.
[39] S. Umemoto, N. Okui, *Polymer* **2001**, *43*, 1423.
[40] Z. Jiajia, Y. Feng, S. Lin, Y. Zhuo, N. G. Guangshun, Chen, Shaoyu, *J. Appl. Polym. Sci.* **2012**, *124*, 452.
[41] A. Chaos, A. Sangroniz, J. Fernández, J. del Río, M. Iriarte, J. R. Sarasua, A. Etxeberria, *J. Appl. Polym. Sci.* **2020**, *137*, 1.
[42] Á. Agüero, E. Corral Perianes, S. S. Abarca de las Muelas, D. Lascano, M. de la Fuente García-Soto, M. A. Peltzer, R. Balart, M. P. Arrieta, *Polymer* **2023**, *15*, 285.
[43] H. Celebi, E. Gunes, *J. Appl. Polym. Sci.* **2018**, *135*, 1.

SUPPORTING INFORMATION

Additional supporting information can be found online in the Supporting Information section at the end of this article.

How to cite this article: B. Tsegaye, K. Westerberg, A. Ström, M. S. Hedenqvist, *J. Appl. Polym. Sci.* **2024**, *141*(38), e55958. https://doi.org/10.1002/app.55958